



## OPEN ACCESS

## EDITED BY

Thierry Massfelder,  
Institut National de la Santé et de la  
Recherche Médicale (INSERM), France

## REVIEWED BY

Matteo Ferro,  
European Institute of Oncology (IEO), Italy  
Gabriel Tao,  
Merck, United States

## \*CORRESPONDENCE

Pengcheng Luo

✉ pluo@whu.edu.cn

Lili Li

✉ 26061047@qq.com

Min Peng

✉ mpeng320@whu.edu.cn

<sup>†</sup>These authors have contributed  
equally to this work

## SPECIALTY SECTION

This article was submitted to  
Genitourinary Oncology,  
a section of the journal  
Frontiers in Oncology

RECEIVED 18 June 2022

ACCEPTED 14 March 2023

PUBLISHED 29 March 2023

## CITATION

Xiong X, Chen C, Li X, Yang J, Zhang W,  
Wang X, Zhang H, Peng M, Li L and Luo P  
(2023) Identification of a novel defined  
inflammation-related long noncoding RNA  
signature contributes to predicting  
prognosis and distinction between the cold  
and hot tumors in bladder cancer.  
*Front. Oncol.* 13:972558.  
doi: 10.3389/fonc.2023.972558

## COPYRIGHT

© 2023 Xiong, Chen, Li, Yang, Zhang, Wang,  
Zhang, Peng, Li and Luo. This is an open-  
access article distributed under the terms of  
the [Creative Commons Attribution License  
\(CC BY\)](https://creativecommons.org/licenses/by/4.0/). The use, distribution or  
reproduction in other forums is permitted,  
provided the original author(s) and the  
copyright owner(s) are credited and that  
the original publication in this journal is  
cited, in accordance with accepted  
academic practice. No use, distribution or  
reproduction is permitted which does not  
comply with these terms.

# Identification of a novel defined inflammation-related long noncoding RNA signature contributes to predicting prognosis and distinction between the cold and hot tumors in bladder cancer

Xi Xiong<sup>1†</sup>, Chen Chen<sup>1†</sup>, Xinxin Li<sup>2†</sup>, Jun Yang<sup>3</sup>, Wei Zhang<sup>3</sup>,  
Xiong Wang<sup>4</sup>, Hong Zhang<sup>4</sup>, Min Peng<sup>5\*</sup>, Lili Li<sup>6\*</sup>  
and Pengcheng Luo<sup>1\*</sup>

<sup>1</sup>Department of Urology, Wuhan Third Hospital School of Medicine, Wuhan University of Science Technology, Wuhan, China, <sup>2</sup>Department of Urology, Wuhan Third Hospital and Tongren Hospital of Wuhan University, Wuhan, China, <sup>3</sup>Department of Urology, Wuhan Third Hospital, Wuhan, China, <sup>4</sup>Department of Pharmacy, Wuhan Third Hospital, Wuhan, China, <sup>5</sup>Department of Oncology, Renmin Hospital of Wuhan University, Wuhan, China, <sup>6</sup>Central Laboratory, Renmin Hospital of Wuhan University, Wuhan, China

**Purpose:** Bladder cancer (BLCA) is one of the most frequently diagnosed urological malignancies and is the 4th most common cancer in men worldwide. Molecular targets expressed in bladder cancer (BLCA) are usually used for developing targeted drug treatments. However, poor prognosis and poor immunotherapy efficacy remain major challenges for BLCA. Numerous studies have shown that long non-coding RNAs (LncRNAs) play an important role in the development of cancer. However, the role of LncRNAs related to inflammation in BLCA and their prognostic value remain unclear. Therefore, this study is aimed to explore new potential biomarkers that can predict cancer prognosis.

**Methods:** We downloaded BLCA-related RNA sequencing data from The Cancer Genome Atlas (TCGA) and searched for inflammation-related prognostic long non-coding RNAs (LncRNAs) by univariate Cox (uniCox) regression and co-expression analysis. We used the least absolute shrinkage and selection operator (LASSO) analysis to construct an inflammation-related LncRNA prognosis risk model. Samples were divided into high-risk score (HRS) group and low-risk score (LRS) group based on the median value of risk scores. The independent variable factors were identified by univariate Cox (uni-Cox) and multivariate Cox (multi-Cox) regression analyses, and receiver operating characteristic (ROC) curves were used to compare the role of different factors in predicting outcomes. Nomogram and Calibration Plot were generated by the R package rms to analyze whether the prediction results are correct and show good consistency. Correlation coefficients were calculated by Pearson analysis. The Kaplan-Meier method was used to assess the prognostic value. The expression of 7 LncRNAs related with inflammation was also confirmed by qRT-PCR in BLCA cell lines. Kyoto Encyclopedia of Gene and

Genome (KEGG) pathways that were significantly enriched ( $P < 0.05$ ) in each risk group were identified by the GSEA software. The R package pRRophetic was used to predict the IC50 of common chemotherapeutic agents. TIMER, XCELL, QUANTISEQ, MCPOUNTER, EPIC and CIBERSORT were applied to quantify the relative proportions of infiltrating immune cells. We also used package ggpubr to evaluate TME scores and immune checkpoint activation in LRS and HRS populations. R package GSEABase was used to analyze the activity of immune cells or immune function. Different clusters of principal component analysis (PCA), t-distribution random neighborhood embedding (t-SNE), and Kaplan-Meier survival were analyzed using R package Rtsne's. The R package ConsensusClusterPlus was used to class the inflammation-related lncRNAs.

**Results:** In this study, a model containing 7 inflammation-related lncRNAs was constructed. The calibration plot of the model was consistent with the prognosis prediction outcomes. The 1-, 3-, and 5-year ROC curve (AUC) were 0.699, 0.689, and 0.699, respectively. High-risk patients were enriched in lncRNAs related with tumor invasion and immunity, and had higher levels of immune cell infiltration and immune checkpoint activation. Hot tumors and cold tumors were effectively distinguished by clusters 2 and 3 and cluster 1, respectively, which indicated that hot tumors are more susceptible to immunotherapy.

**Conclusion:** Our study showed that inflammation-related lncRNAs are closely related with BLCA, and inflammation-related lncRNA can accurately predict patient prognosis and effectively differentiate between hot and cold tumors, thus improving individualized immunotherapy for BLCA patients. Therefore, this study provides an effective predictive model and a new therapeutic target for the prognosis and clinical treatment of BLCA, thus facilitating the development of individualized tumor therapy.

#### KEYWORDS

bladder cancer, inflammation, lncRNA, prognosis, immune

## 1 Introduction

Bladder cancer (BLCA) is a common cancer with high morbidity and mortality rates worldwide. Most BLCA patients are often diagnosed in the late stages and lack effective treatments (1, 2). There were about 81,400 new BLCA cases and 17,980 BLCA deaths in the United States in 2020 alone. Due to the poor selectivity and side effects of traditional treatments, new treatment strategies are urgently needed for BLCA (3). Immunotherapy is increasingly used in the treatment of malignant tumors, particularly advanced BLCA. Although immunotherapy with immune checkpoint inhibitors (ICIs) can greatly increase the survival rate and duration of response, only a few patients respond to ICIs (4). Therefore, finding an effective immunotherapy for BLCA patients remains a key direction of research.

Previous studies have shown that many malignant tumors are caused by infection, which along with inflammation accounts for 25% of the causes of cancer (5, 6). Persistent infection during chronic inflammation can cause cell DNA damage and tissue damage and repair, leading to genomic changes and hence tumor development.

Chronic inflammation is characterized by persistent neutrophil infiltration, which is also a feature of the tumor microenvironment (TME). Neutrophils can promote tumorigenesis by inhibiting adaptive immune responses in the TME (7). It has been reported that inflammation is the initiating factor for TME. Macrophages are important components of tumor immune cells and can promote tumorigenesis and tumor development (8). M1 macrophages promote type I immune response by secreting pro-inflammatory cytokines (9, 10), whereas M2 macrophages promote tumor progression by producing T helper 2 (Th2) cytokines (11, 12). Based on these findings, we hypothesize that inflammation-related genes may be potential molecular targets for BLCA treatment.

The role of long non-coding RNAs (lncRNAs) in cancer progression has been increasingly investigated in recent years. lncRNAs are > 200 bp in length and widely distributed throughout the genome. They play a key role in diverse biological and physiological processes, including epigenetic control, cell cycle regulation, and cell differentiation (13). lncRNAs have also been shown to be involved in inflammation-related diseases (14). The inflammatory TME is the key to most tumors progressing from

controllable inflammation to uncontrollable inflammation. Therefore, inflammation-related lncRNAs may play a pivotal role in the transition to inflammatory TME during tumor development (15–17). According to research, lncRNA-PDPK2P promotes hepatocellular carcinoma (HCC) progression *via* the PDK1/Akt/Casepase-3 signaling pathway, and PDPK2P expression can be used as a prognostic marker for HCC (18). However, the role of inflammation-related lncRNAs in BLCA treatment is yet to be examined. Here, we investigated the effectiveness of inflammation-related lncRNAs in classifying cold and hot tumors to improve the efficacy of immunotherapy and provide potential biomarkers for the selection of immunotherapy in BLCA patients (19).

## 2 Materials and methods

### 2.1 Data collection

A workflow for this study is summarized in Figure 1. RNA-seq data and clinical characteristics were acquired from the TCGA (<https://portal.gdc.cancer.gov/>), including 19 normal bladder samples and 414 BLCA samples. Perl was used to combine the individual RNA-seq data by sample ID. A total of 14,056 lncRNAs were identified in the BLCA cohort. Patients with short or missing overall survival (OS; <30 days) were excluded.

### 2.2 Acquisition of inflammation-related lncRNAs

A total of 200 inflammation-related genes were downloaded from the Molecular Signatures Database (<http://www.gsea-msigdb.org/gsea/index.jsp>) (Supplementary Table 2). The correlation between the 14,056 lncRNAs and the 200 inflammation-related genes in BLCA was determined using the Spearman approach (20). lncRNAs with a correlation coefficient of > 0.4 and  $P < 0.001$  were defined as inflammation-related lncRNAs. Differentially

expressed inflammation-related lncRNAs were identified by  $|\log_2 FC| > 1$  and  $P < 0.05$  using the R package Limma.

### 2.3 Prognostic model construction and LASSO regression analysis

To determine the stability and accuracy of the prognosis, we analyzed the 1,041 inflammation-related lncRNAs by uniCox regression and removed overfitting variables using LASSO regression. A PRS model was constructed to accurately predict overall survival rate (OS) of BLCA samples. The ideal values for the penalty parameters were identified after 10 cross-validations to build the inflammation-related lncRNAs-based prognostic model (21). The 1-, 3-, and 5-year receiver operating characteristic (ROC) curves of the model were constructed. The risk score was calculated by: Risk score  $\sum_{i=1}^n \text{coef}(i) \times \text{expr}(i)$ , where  $\text{expr}(i)$  is the relative mRNA expression of the gene in every patient  $i$ , and  $\text{coef}(i)$  is the LASSO coefficient of the gene in every patient  $i$ . The median risk score was used to classify samples into low-risk score (LRS) and high-risk score (HRS) groups. We obtained 400 patients with pertinent clinical information and randomly divided them at 1:1 into the training and test groups using the “caret” package.

### 2.4 Independence factor analysis

Independent factors, including risk scores and clinical parameters, were analyzed by uniCox and multiCox regression analyses. ROC analysis was used to determine the predictive accuracy of each factor.

### 2.5 Construction of nomogram and calibration plot

Nomograms for the 1-, 3-, and 5-year OS rates were generated by the “rms” package based on the risk score and clinical parameters. A

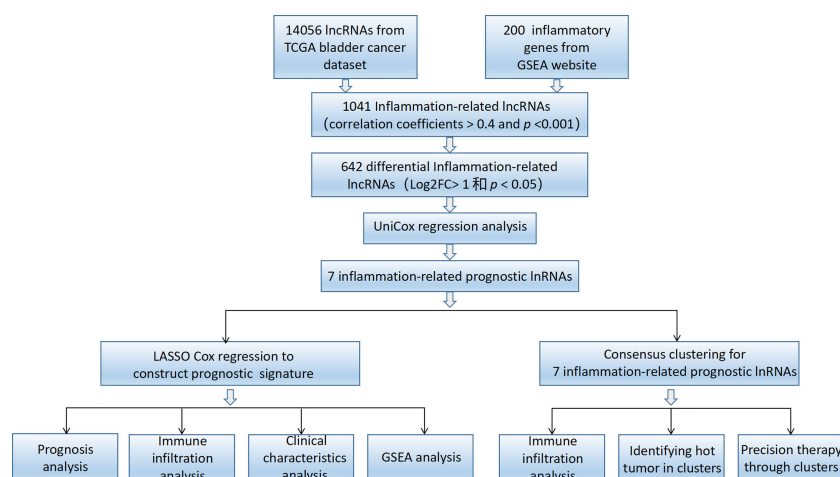


FIGURE 1  
Study workflow.

calibration plot was created to measure the consistency between the predicted outcome and the actual survival rate.

## 2.6 Functional enrichment analysis

Kyoto Encyclopedia of Gene and Genome (KEGG) pathways that were significantly enriched ( $P < 0.05$ ) in each risk group were identified by the GSEA software (<https://www.gsea-msigdb.org/gsea/login.jsp>).

## 2.7 TME and immune checkpoints

The enrichment of immune cytokines in the HRS group were evaluated based on the GSEA results. To evaluate immune cell infiltration, correlations between risk scores and immune checkpoint molecule expression were determined by TIMER, EPIC, MCPcounter, QUANTISEQ, CIBERSORT, XCELL, and CIBERSORT. TME variations in each risk group were analyzed by Limma package and presented in a bubble chart. TME score and immune checkpoint activity were compared between the LRS and HRS groups by the “ggpubr” package.

## 2.8 Prediction of potential compounds for BLCA treatment

IC<sub>50</sub> values of compounds were obtained from the Genomics of Drug Sensitivity in Cancer (GDSC) website (<https://www.cancerrxgene.org/>) to identify candidate drugs for BLCA treatment. Chemicals that may be used for BLCA treatment were predicted using the R packages pRRophetic, limma, ggpub, and ggplot2 (22).

## 2.9 Consensus clustering by seven inflammation-related prognostic lncRNAs

To study BLCA response to immunotherapy, BLCA patients were divided into subgroups by the “ConsensesClusterPlus” package, and the immunotherapy responses in these subgroups were determined based on the lncRNA expression levels. Principal component analysis (PCA), Kaplan–Meier estimation, and t-distributed stochastic neighbor embedding (t-SNE) were performed by the “Rtsne” package, and immunoassay and drug sensitivity analyses were performed by “Limma”, “scales”, and “pRRophetic” packages.

## 2.10 Cell culture

Sv-huc-1, T24, and 5637 cell lines were purchased from IMMOCELL (Xiamen, Fujian, China) and respectively cultured in DMEM-F12K medium, McCoy’s 5A medium, and RPMI-1640

medium containing 1% streptomycin-penicillin and 10% FBS (Gibco) at 37°C.

## 2.11 RNA extraction and qRT-PCR

Total RNA extraction was performed on the three cell lines using the RNA Isolation Kit (R6934-01, Omega Bio-Tek, USA) as per the manufacturer’s protocol. Total RNA concentration and purity were determined by absorbance readings at 260 nm with a spectrophotometer (Quawell UV Spectrophotometer Q3000). RNA was reversely transcribed into cDNA using the TOYOBO ReverTra Ace qPCR RT kit, and amplified by real-time PCR using the Bio-Rad CFX Manager system. Expression levels of AC068196.1, LNCAROD, MAP3K14-AS1, AC021321.1, LINC02256, NR2F1-AS1, and KCNQ10T1 were calculated by the  $2^{-\Delta\Delta C_q}$  method (23). Primers are shown in [Supplementary Table 1](#).

## 2.12 Statistic analysis

Spearman correlation analysis was employed to calculate correlation coefficients. Using the Kaplan–Meier method, the Cox regression model, and log-rank test, the prognostic value was evaluated. The Wilcoxon rank-sum test was utilized to compare the two groups. Three or more groups were compared by the Kruskal–Wallis test. Two-tailed  $P < 0.05$  indicated significant difference.

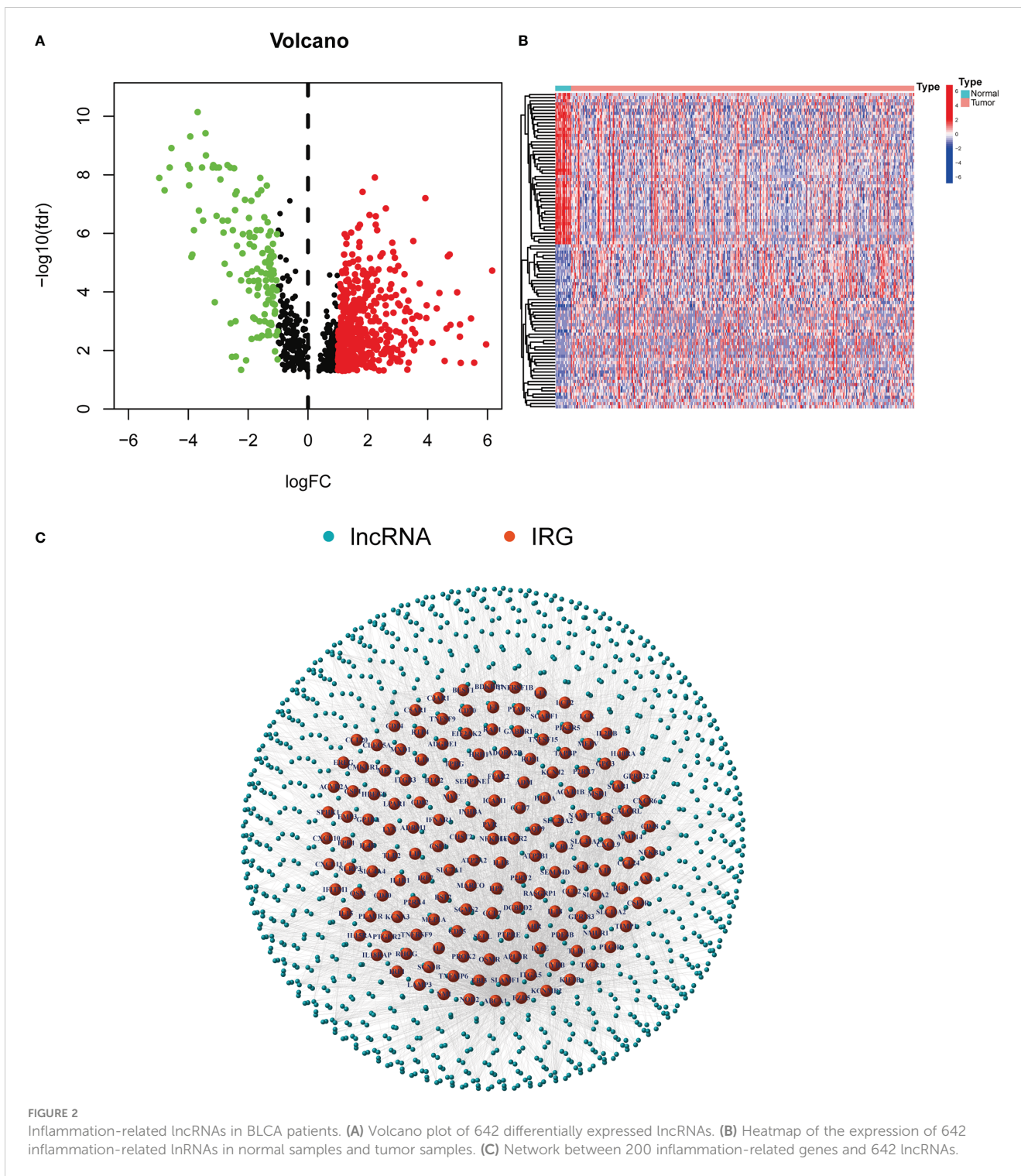
# 3 Results

## 3.1 Identification of inflammation-related lncRNAs in BLCA

A workflow of this study is shown in [Figure 1](#). The RNA-seq data of 433 samples, including 19 normal samples and 414 BCLA samples, and their corresponding 412 clinical files were analyzed. A total of 1,041 inflammation-related lncRNAs were identified through correlation analysis of the expression of 14,056 lncRNAs and the mRNA expression of 200 inflammation-related genes. 642 differentially expressed inflammation-related lncRNAs, including 515 upregulated and 127 downregulated lncRNAs, were identified ([Figure 2A](#)). The heatmap results revealed that BLCA patients could be clearly divided into two distinct groups ([Figure 2B](#)). The correlations between the 200 inflammation-related genes and 642 lncRNAs are shown in [Figure 2C](#); [Supplementary Table 3](#).

## 3.2 Prognostic signature construction and validation

To prevent overfitting of the prognostic signature, We performed lasso regression on these lncRNAs and extracted 7 lncRNAs related to inflammation in BLCA, when the first-order value of  $\text{Log}(\lambda)$  was the least probable deviation ([Figures 3A, B](#)). We



used the following formula to calculate the risk score:  $AC068196.1 \times (-2.68949664829451) + LNCAROD \times (0.313548802975356) + MAP3K14-AS1 \times (-0.936638242135287) + AC021321.1 \times (-0.746810149653322) + LINC02256 \times (1.412877497541) + NR2F1-AS1 \times (0.563351996798577) + KCNQ1OT1 \times (2.09002192071773)$  (24). 7 inflammation-related lncRNAs were

markedly correlated with OS as determined by uniCox regression (all  $P < 0.05$ ) and made a heatmap (Figures 3C, D). In addition, The Sankey diagram revealed that 7 lncRNAs were upregulated (Figure 3E). Furthermore, using the risk score formula, the distribution of risk scores, survival status, survival time, and the related expression criteria of these lncRNAs were compared between the LRS and HRS

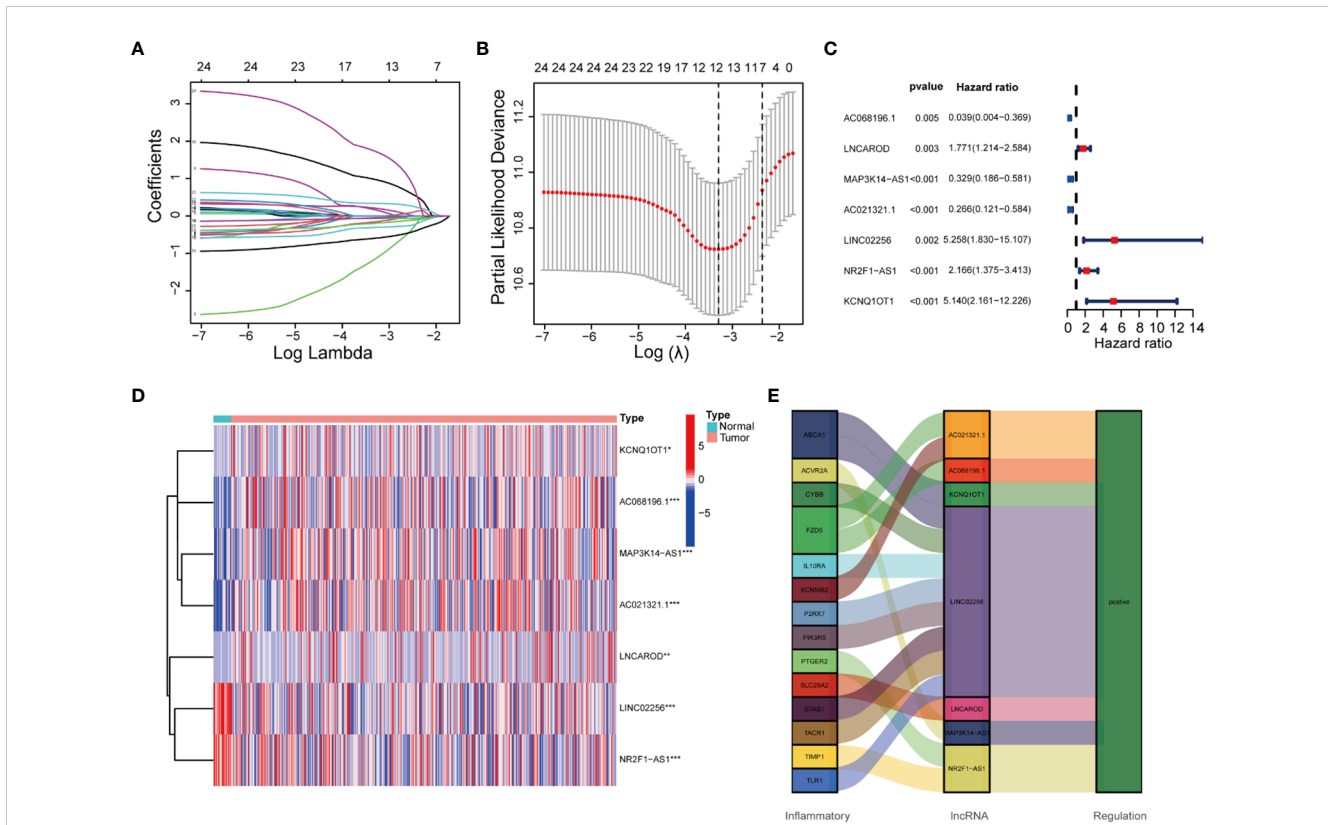


**FIGURE 3** Construction of the 7 inflammation-related lncRNAs model. Cox regression analysis of inflammation-related lncRNAs in BLCA. (A) 10-fold cross-validation in the LASSO analysis. (B) LASSO coefficient profile of the 7 inflammation-related lncRNAs. (C) Univariate Cox regression analysis. (D) Heatmap of the expression profiles of 7 lncRNAs. (E) The Sankey diagram of inflammatory genes and lncRNAs.

groups of patients in the train, test, and entire sets, which revealed that the patients in the high-risk group had low overall survival rate and worse prognosis (Figure 4).

### 3.3 lncRNA expression in BLCA cell lines

Furthermore, we validated expression of the 7 inflammation-related lncRNAs in the normal bladder cell (SV-HUC-1), and BLCA cells (T24 and 5637) by qRT-PCR. The expression level of AC021321.1, AC068196.1 showed no difference between T24 cell line and SV-HUC-1. The expression level of LNCAROD, LINC02256, NR2F1-AS1, MAP3K14-AS1, and KCNQ1OT were significantly higher in the BLCA cell lines than in SV-HUC-1 cells (Figure 5).

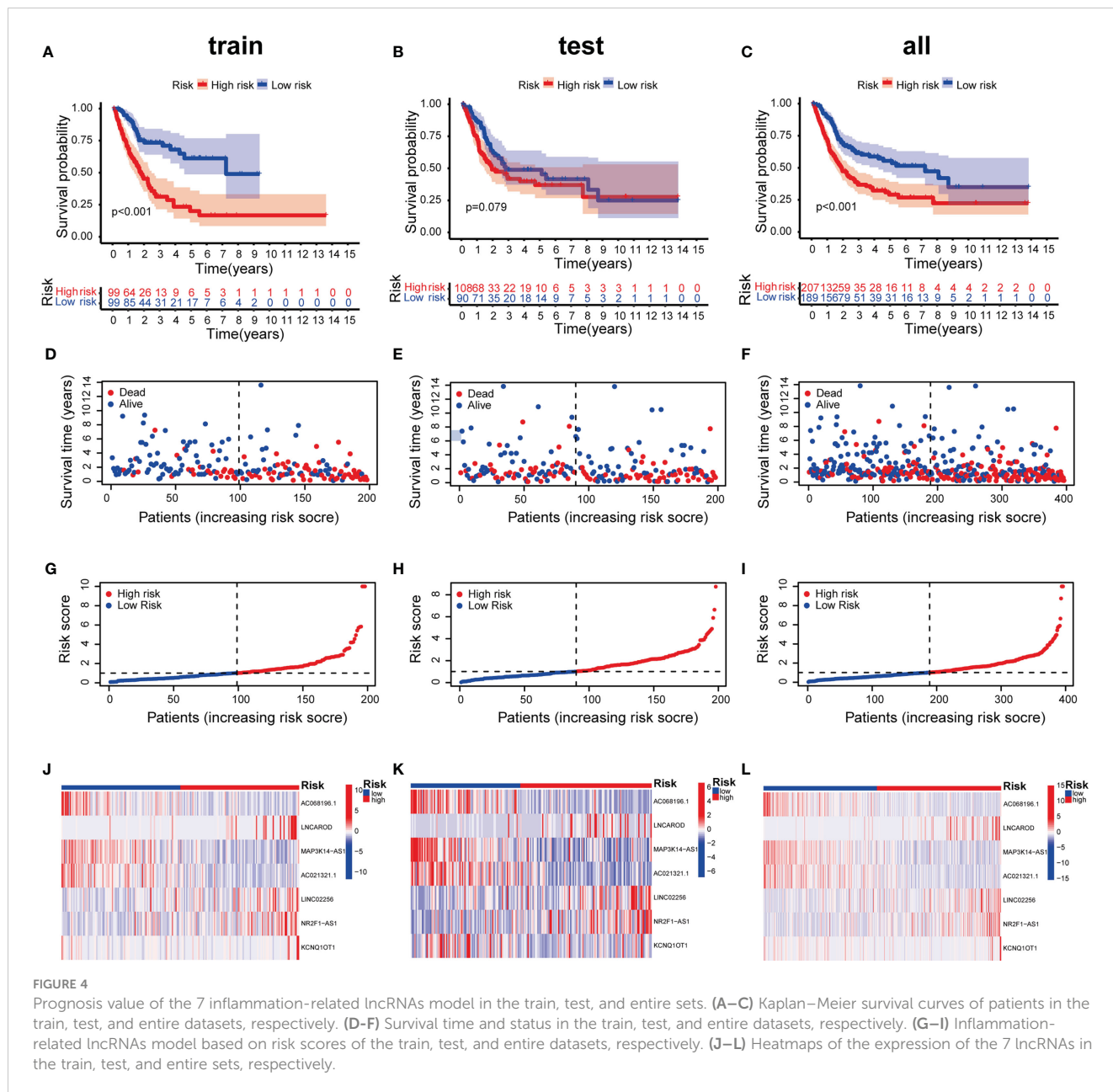
### 3.4 Cox analysis and nomogram construction

UniCox regression revealed significant differences in risk scores (HR=1.051 and 95%CI [1.034-1.067],  $P < 0.001$ ), age (HR=1.030, 95%CI [1.014-1.047],  $P < 0.001$ ) and stage (HR=1.675, 95%CI [1.372-2.044];  $P < 0.001$ ) (Figure 6A). MultiCox regression also showed significant differences in risk scores (HR=1.048 and 95%CI [1.031-1.065],  $P < 0.001$ ), age (HR=1.030 and 95%CI [1.014-1.047],

$P < 0.001$ ) and stage (HR=1.675 and 95%CI [1.372-2.044],  $P < 0.001$ ) (Figure 6B), indicating that risk score, age, and stage were three independent prognostic factors for BLCA. Furthermore, the ROC AUC of the 1-, 3-, and 5-year OS rates was 0.699, 0.689, and 0.699, respectively, which demonstrated that the constructed model accurately predicted the OS rate of BLCA patients (Figure 6C). By combining the results of the constructed model with clinical traits, it was revealed that the risk score has a significantly higher AUC than other clinical traits, indicating that risk score was superior to other clinical traits in OS prediction for BLCA patients (Figure 6D). OS rates of stages I-II and stages III-IV BLCA patients were significantly lower in the HRS group than in the LRS group (Figures 6E, F). It indicated that patients with different staging had significantly lower survival rates in the HRS group than in the LRS group. A nomogram was further constructed to predict the 1-, 3-, and 5-year OS of BLCA patients (Figure 6G), We also utilized the 1-, 3-, and 5-year calibration plots to attest that the nomogram had a good concordance with the prediction of 1-,3-, and 5-year OS (Figure 6H).

### 3.5 GSEA

In order to study the differences in biological functions between risk groups, we used GSEA software to explore HRS groups across the entire set KEGG pathway. The GSEA of the HRS group showed



that the majority of the top 10 enriched KEGG pathways were related with tumor immunity and invasion, including “chemokine signal pathway” and “leukocyte transendothelial migration” (Figure 7; Supplementary Figure 1). Therefore, we attempted to perform immune analysis in the model.

### 3.6 Immune cell and drug sensitivity analyses

Immune cell bubble plots showed that more immune cells are related with HRS populations on different databases (Figure 8A). The correlation of immune cells calculated on different platforms indicated that the risk score was positively correlated with Neutrophil TIMER, Myeloid dendritic cell\_TIMER,

Monocyte\_XCELL, Macrophage M1\_QUANTISEQ, T cell CD8+\_TIMER, and Macrophage M1\_XCELL, Macrophage\_XCELL ( $P < 0.05$ ) (Figure 8B; Supplementary Table 4). ssGSEA revealed higher relative frequency of immune cells and better immune functions in the HRS group than in the LRS group (Figures 8C, D). The HRS group had higher immune cell scores, stromal cell scores, and ESTIMATE scores, indicating greater immune cell infiltration (Figure 9A). It was also found that both immune cell infiltration and ICI activation were higher in the HRS group (Figure 9B) (25). We can select appropriate checkpoint inhibitors for BLCA patients who can be grouped according to risk patterns. The  $IC_{50}$  values of nine immunotherapeutic, chemical, and targeted agents, such as AUY922 and BMS.509744, were lower in the HRS group, demonstrating that the HRS group responded better to these treatments (Figure 10).

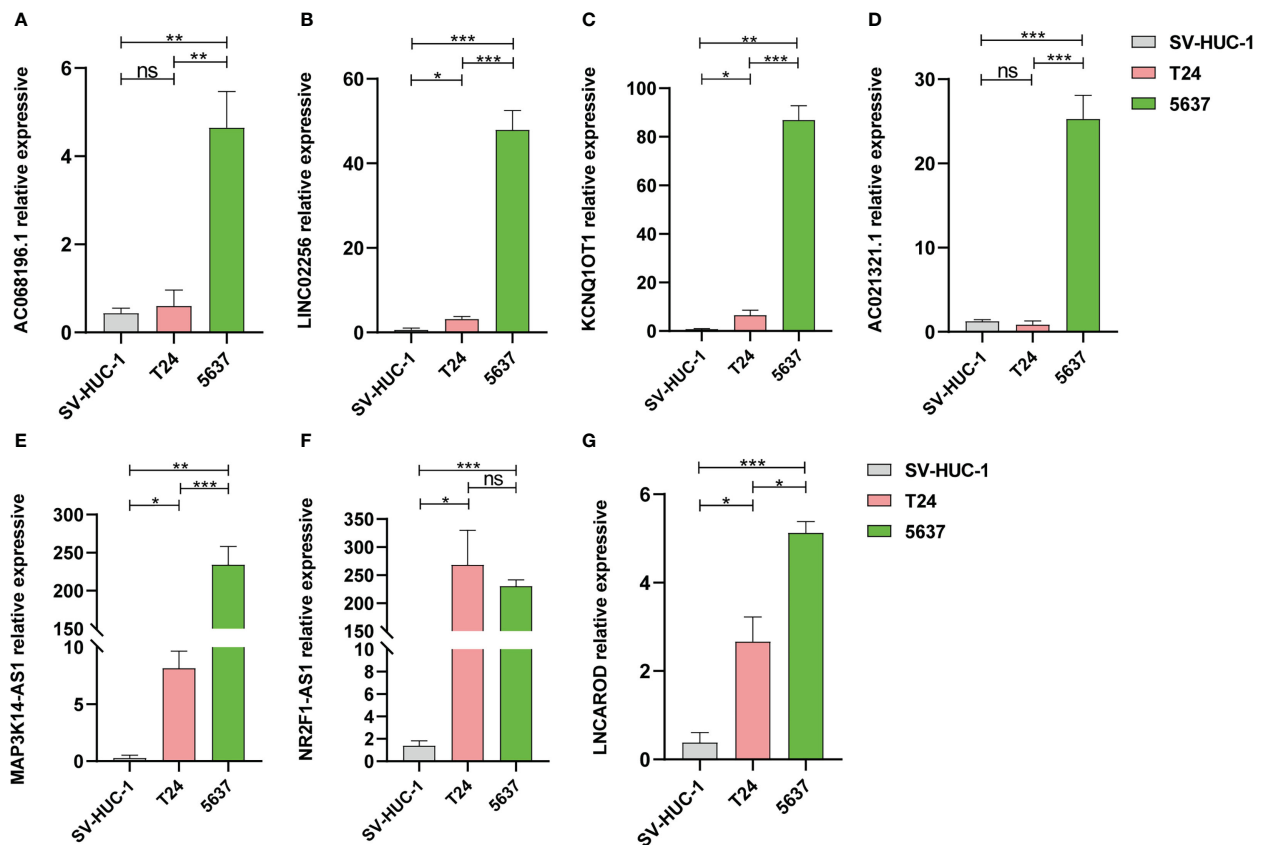


FIGURE 5

The mRNA expression levels of 7 lncRNAs in two bladder cancer cell lines by qRT-PCR. (A) AC068196.1; (B) LINC02256; (C) KCNQ1OT1; (D) AC021321.1; (E) MAP3K14-AS1; (F) NR2F1-AS1; (G) LNCAROD. \* $p < 0.05$ , \*\* $p < 0.01$ , and \*\*\* $p < 0.001$ . ns, not statistically significant.

### 3.7 Consensus clustering and precision therapy

The patients were grouped into 3 clusters according to inflammation-related lncRNAs expression (Figure 11A) (26). The three clusters were clearly distinguished by PCA (Figure 11B) and t-SNE analysis (Figure 11C), and the two risk groups were distinctly separated by PCA (Figure 11D). The OS rate was higher in cluster 1 than in clusters 2 and 3 ( $P < 0.001$ ) (Figure 11E), and most BLCA patients in cluster 1 belonged to the LRS group, while most BLCA patients in clusters 2 and 3 belonged to the HRS group (Figure 11F). The immune and stromal cell scores of cluster 3 were the highest among the three clusters, and the immune score of cluster 2 was higher than that of cluster 1, which was consistent with the results of the Sankey diagram, and indicated a greater extent of immune cell infiltration in the HRS group. In addition, our data showed that TME varied among different clusters (Figure 11G), and immune cell infiltration was greater in clusters 2 and 3 (Figure 12A; Supplementary Table 5). The expression of most ICIs decreased as cluster number increased (cluster 1 < cluster 2 < cluster 3), including IDO1, CD274 (PD-L1), HAVCR2 (TIM3), and LAG3 (Figure 12B), which were highly effective therapeutic targets for hot

tumors. We then classified clusters 2 and 3 as “hot” tumors and cluster 1 as a “cold” tumor based on their TME and responses to immunotherapy (27). It was found that clusters 2 and 3 (hot tumors) were highly associated with cell infiltration and more sensitive to immunotherapy. By comparing drug sensitivity, we discovered that 14 immunotherapeutic, chemical, or targeted agents, including AUY922, had lower  $IC_{50}$  values in clusters 2 and 3 (Figure 12C; Supplementary Figure 2B), which indicated that hot tumors responded better to these treatments.

## 4 Discussions

At present, BLCA is still a major global health concern, with a prevalence of about 500 to 50,000 new cases each year (28). BLCA is a highly differentiated cancer with a poor prognosis (29), and the 5-year OS rate for all BLCA stages is still less than 20% (30). Once the tumor reaches the locally advanced or metastatic stage, conventional chemotherapy treatments for BLCA are no longer effective (31). There is an urgent need for new diagnostic and therapeutic methods to assess the prognosis of bladder cancer and to provide guidance for individualized clinical treatment. Clinical



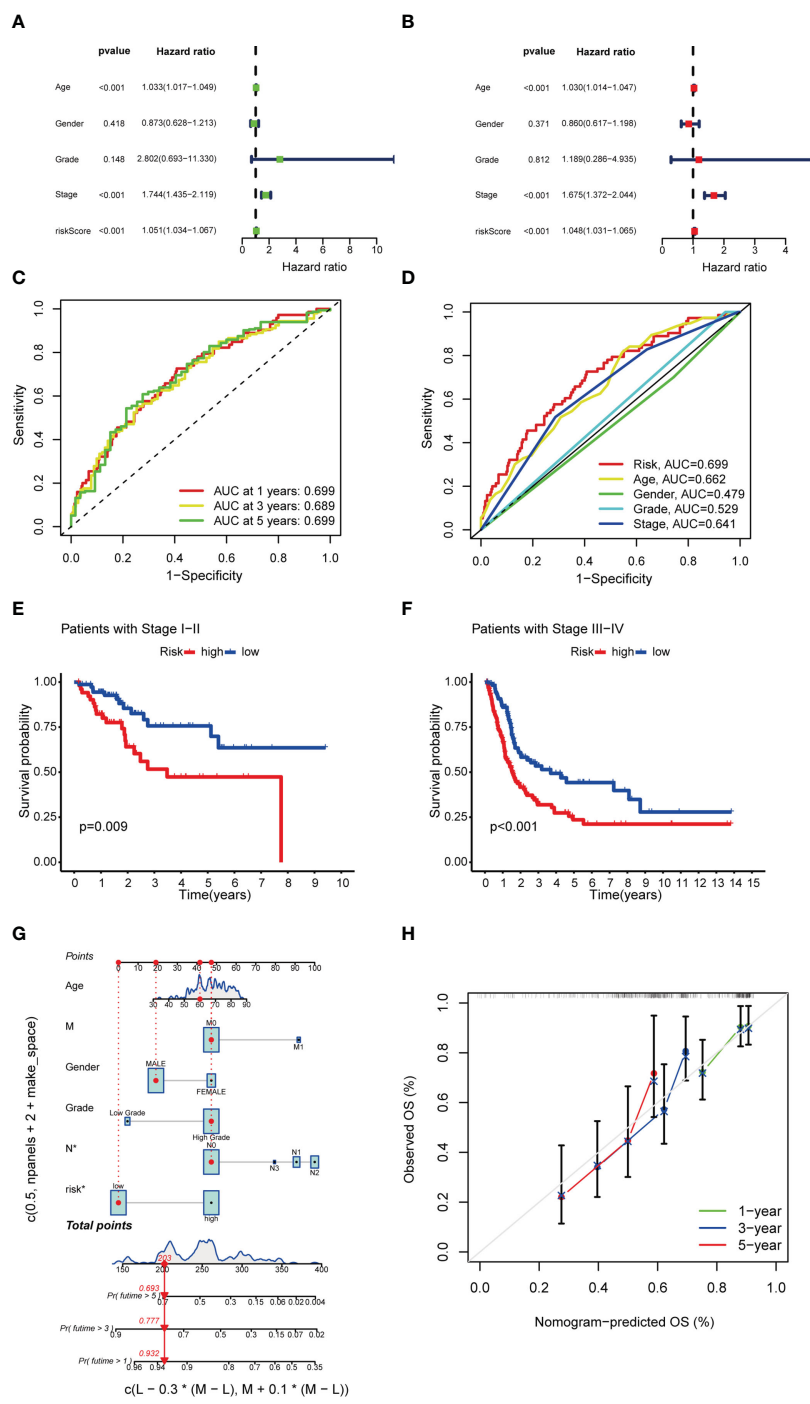


**FIGURE 6** Univariate Cox and multivariate Cox regression analyses and nomogram construction. **(A, B)** Univariate Cox **(A)** and multivariate Cox **(B)** analyses of clinical factors and risk score for prediction of overall survival. **(C, D)** 1-, 3-, and 5-year ROC curves of risk score and clinical characteristics. **(E, F)** Kaplan–Meier survival curves of patients in the stage I–II and stage III–IV groups, respectively. **(G)** 1-, 3-, and 5-year overall survival predicted by the nomogram integrating risk score, age, and tumor staging. **(H)** Calibration curves for 1-, 3-, and 5-year overall survival.

biomarkers of urine in liquid biopsies have been shown to be useful in the diagnosis and prognosis of bladder cancer. Urine is easy to obtain, does not require special patient compliance, and has a simple composition, making it highly useful for clinical practice (32). In addition, ICIs have demonstrated to be effective treatments

for BLCA and other malignant tumors. However, only a small number of patients have a lasting response to ICIs, and hence it is vital to identify more accurate response indicators to improve the efficacy of immunotherapy (33). Invasive tumors with high immune scores are known as “hot tumors”, whereas non-invasive tumors

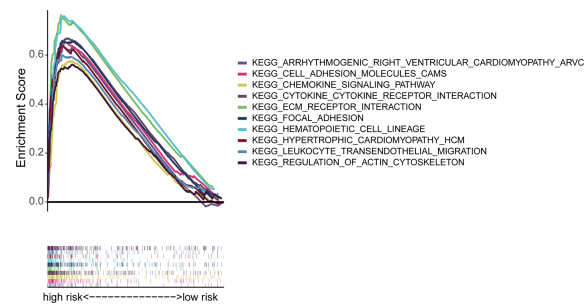


FIGURE 7  
Enrichment of immune cytokines in the top 10 pathways in the high-risk group.

with low immune scores are known as “cold tumors”. For example, tumors with high expression of MHC class I and immune checkpoints are called “hot tumors”. However, ICIs are only effective for hot tumors and essentially ineffective for cold tumors (34). T cell targeted immunotherapy and other immunotherapeutic drugs can be used for the treatment of hot tumors. On the other hand, cold tumors, also known as immunosuppressive tumors, are difficult to be recognized by immune cells, resulting in fewer T cells infiltrating into and around the tumor (35, 36). CD8<sup>+</sup> T cells are activated by tumor antigens and infiltrate the tumor. The application of anti-PD-1/PD-L1 antibodies can significantly enhance the efficacy of immunotherapy (34). In order to enhance anti-tumor immunity, immunotherapy alone is far from enough. Transforming cold tumors into hot tumors will be pivotal to improve the efficacy of immunotherapy (35).

In this study, we constructed a prognostic model using 7 inflammation-related lncRNAs. The new model classified patients into two groups, namely the HRS group and the LRS group, which were then subjected to Kaplan-Meier analysis, ROC analysis, GSEA analysis, and IC50 prediction. Our results showed that the risk group can serve as a guide for clinical evaluation and prognosis prediction, but cannot effectively distinguish hot tumors from cold tumors. We also observed that BLCA patients can be divided into different subtypes based on gene expression clustering. Each tumor subtype has a different TME, prognosis, and immune response (27). By dividing these lncRNAs into three groups through consensus clustering, we observed that cluster 1 had less CD8<sup>+</sup> T cell infiltration and an immunosuppressive TME, while clusters 2 and 3 had greater CD8<sup>+</sup> T infiltration, an increased immune score, and PD-L1, LAG3, and TIM3 expression. Therefore, we identified clusters 2 and 3 as “hot tumors” which are more susceptible to immunotherapy drugs (26, 35). It is known that immunotherapy such as anti-programmed death ligand (PD-L)1/PD-1 therapy is more effective for hot tumors. In order to achieve a better tumor response to immunotherapy, various studies have investigated the means of transforming cold tumors into hot tumors (37, 38). Our findings demonstrated that inflammation-related lncRNAs not only serve as prognostic markers that effectively differentiate between

cold and hot tumors, but also provide a theoretical basis for individualized BLCA treatment.

Inflammation is an immune response to infection, trauma, or other stressors, and is crucial for maintaining overall health (39). Chronic inflammation can increase the risk of cancer and promote cancer growth by inducing tumorigenesis, progression, and metastasis (40). A growing number of studies have shown that tumorigenesis may be driven by an inflammatory TME, especially in gastric cancer (41), glioma (42), and colorectal cancer (43, 44). Therefore, inflammation may be a contributing factor to BLCA progression. We generated a 7 lncRNA-based risk marker to explore its correlation with BLCA. The functional roles of some of these selected lncRNAs in cancer progression have been reported in several studies. Jia et al. (45) found that LNCAROD is involved in tumor malignancy and chemoresistance, especially in a hypoxic microenvironment, by increasing PKM2 levels and ultimately aerobic glycolysis in cancer cells. Kuang et al. (46) reported that the lncRNA MAP3K14-AS1 has a prognostic marker for BLCA. Luo et al. (47) showed that NR2F1-AS1 can modulate cancer cell proliferation, invasion, migration, apoptosis, cell cycle, and glycolysis *via* various mechanisms, and is aberrantly expressed in numerous malignancies, which suggests that NR2F1-AS1 may be a potential therapeutic target and prognostic marker for cancer. He et al. (48) demonstrated that KCNQ1OT1 can recruit DNA methyltransferases to the EIF2B5 promoter to downregulate EIF2B5 expression and thereby promote ovarian cancer metastasis.

We calculated individual AUC values for ROC to obtain the most accurate model and the optimal cut-off point for distinguishing HRS and LRS BLCA patients. Kaplan-Meier analysis showed significantly shorter survival in the HRS group. Surprisingly, it was found that risk scores were related with BLCA staging. Furthermore, risk scores were significantly higher in high-grade BLCA patients than in low-grade BLCA patients, and were consistent with prognosis. As a result, we constructed a nomogram that integrates these characteristics to generate accurate predictions of clinical outcomes.

The GSEA of differentially expressed genes (DEGs) between the HRS and LRS groups showed that DEGs in the HRS group were

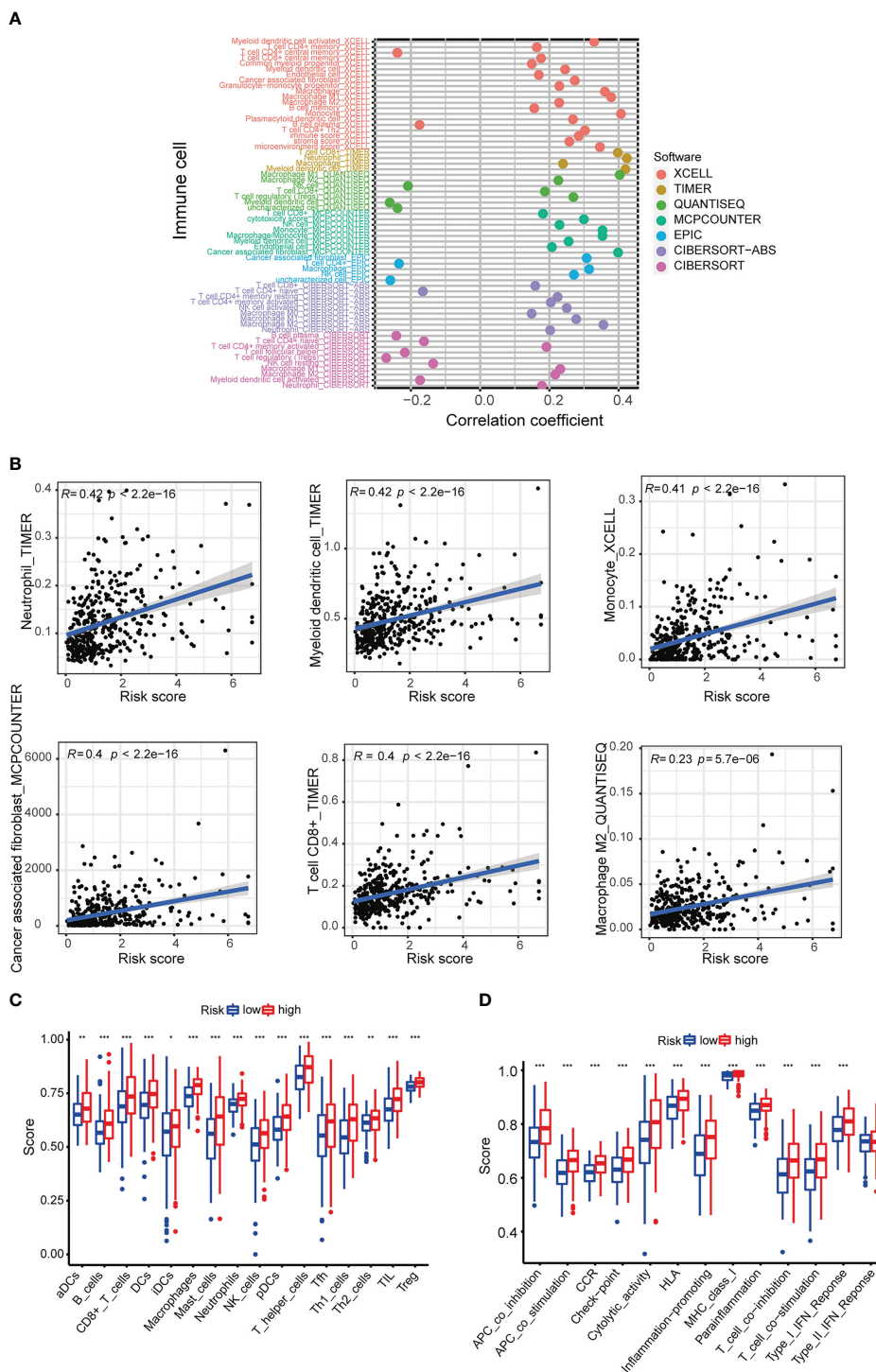


**FIGURE 8** Investigation of tumor immune factors. **(A)** The immune cell bubble of risk groups. **(B)** The correlation between risk score and immune cells. **(C, D)** Relative frequency of immune cells and immunological activities assessed using ssGSE. \* $p < 0.05$ , \*\* $p < 0.01$ , and \*\*\* $p < 0.001$ .

significantly related with the chemokine signal pathway, leukocyte transendothelial migration, extracellular matrix (ECM) receptor signaling, and adherens junction, which are highly correlated with tumor invasion. Moreover, we also calculated the chemosensitivity

of patients based on the  $IC_{50}$  value and screened for candidate small-molecule compounds.

Previous studies have shown that circulating tumor cells play an important role in tumor development and metastasis, and are

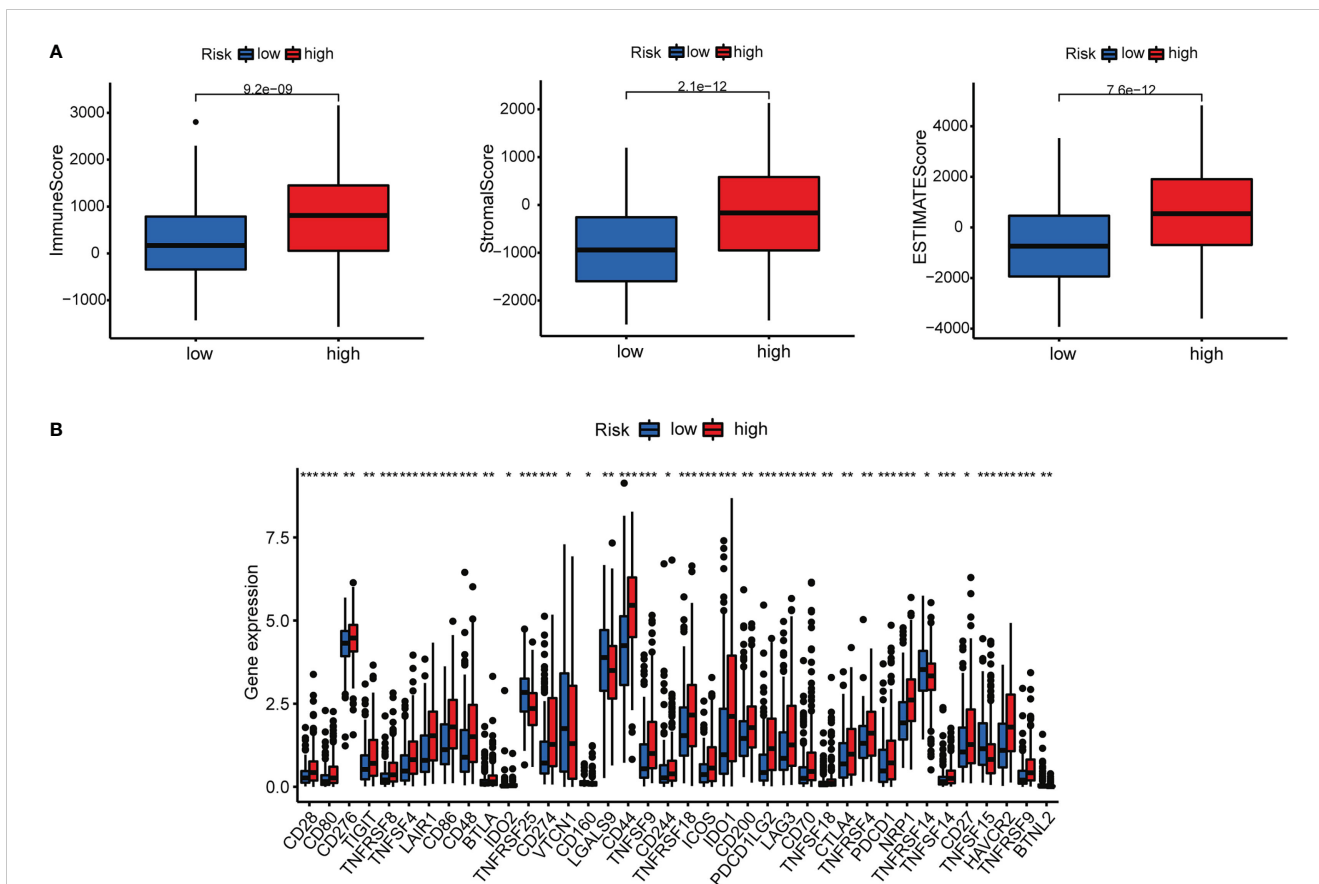


FIGURE 9 Investigation of tumor immunotherapy. (A) Comparison of immune scores between low-risk and high-risk groups. (B) Expression of 18 immune checkpoints in different risk groups. \* $p < 0.05$ , \*\* $p < 0.01$ , and \*\*\* $p < 0.001$ .

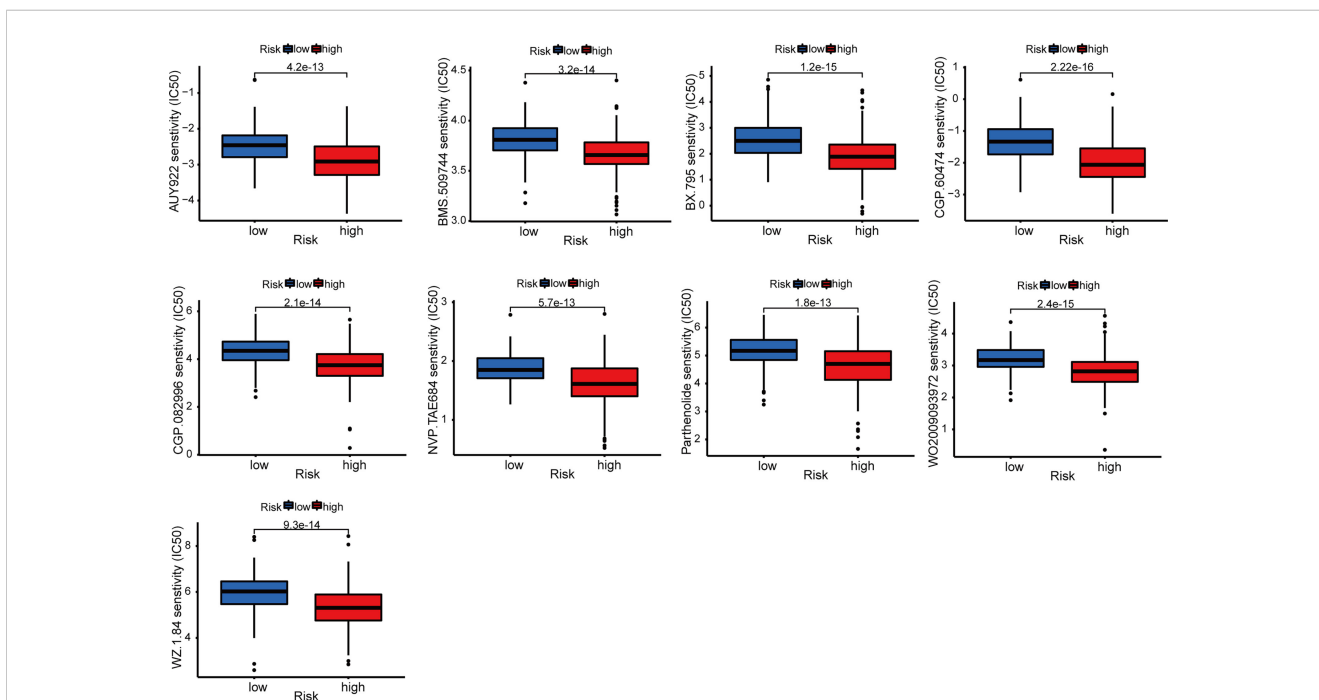
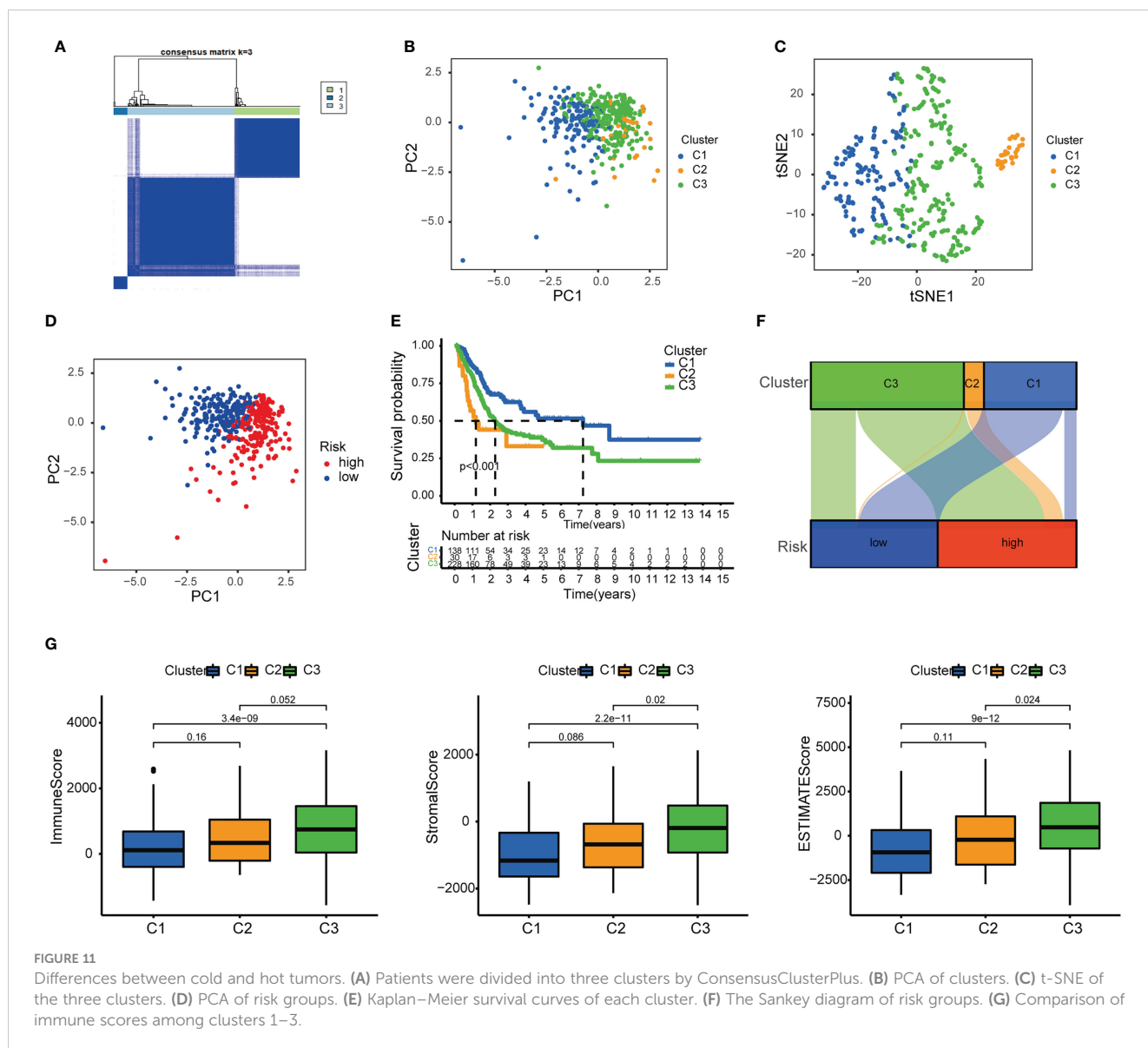


FIGURE 10 Immunotherapy response of risk groups. The IC<sub>50</sub> values of 9 immunotherapeutic, chemical, or targeted agents used in the risk groups.



closely related with survival of BLCA patients. Detection of circulating tumor cells can help assess the prognosis of BLCA patients and guide individualized clinical treatment (49).

Similarly, these inflammation-related lncRNAs can not only be used as prognostic predictors for BLCA prognosis but also provide guidance for clinical drug use, which was helpful for further experimental research and a better understanding of BLCA pathogenesis. However, this study also has several limitations. The risk assessment data of our lncRNAs originated from a public database, and there is a lack of more external transcriptome information to verify the role of these inflammation-related lncRNAs in BLCA. The specific molecular mechanism of inflammation-related lncRNAs in BLCA is not clear, and hence further studies are needed. On the other hand, heterogeneity

among the normal and tumor samples may affect the accuracy of the data analysis. However, the construction of this model only requires tumor samples with clinical information, so it may not affect the accuracy of inflammation-related lncRNAs in predicting BLCA risk. The immune cell results were calculated using different platforms, which can be regarded as an external verification. Collectively, our findings may open new avenues for finding suitable treatment alternatives for BLCA patients, and our model is feasible for future exploration of BLCA pathogenesis and clinical guidance in BLCA treatment. Since both lncRNAs and inflammatory signaling pathways are involved in the progression of tumor cells (50), further understanding of their molecular mechanisms will improve treatment efficacy and reduce treatment-related toxicities in BLCA patients.

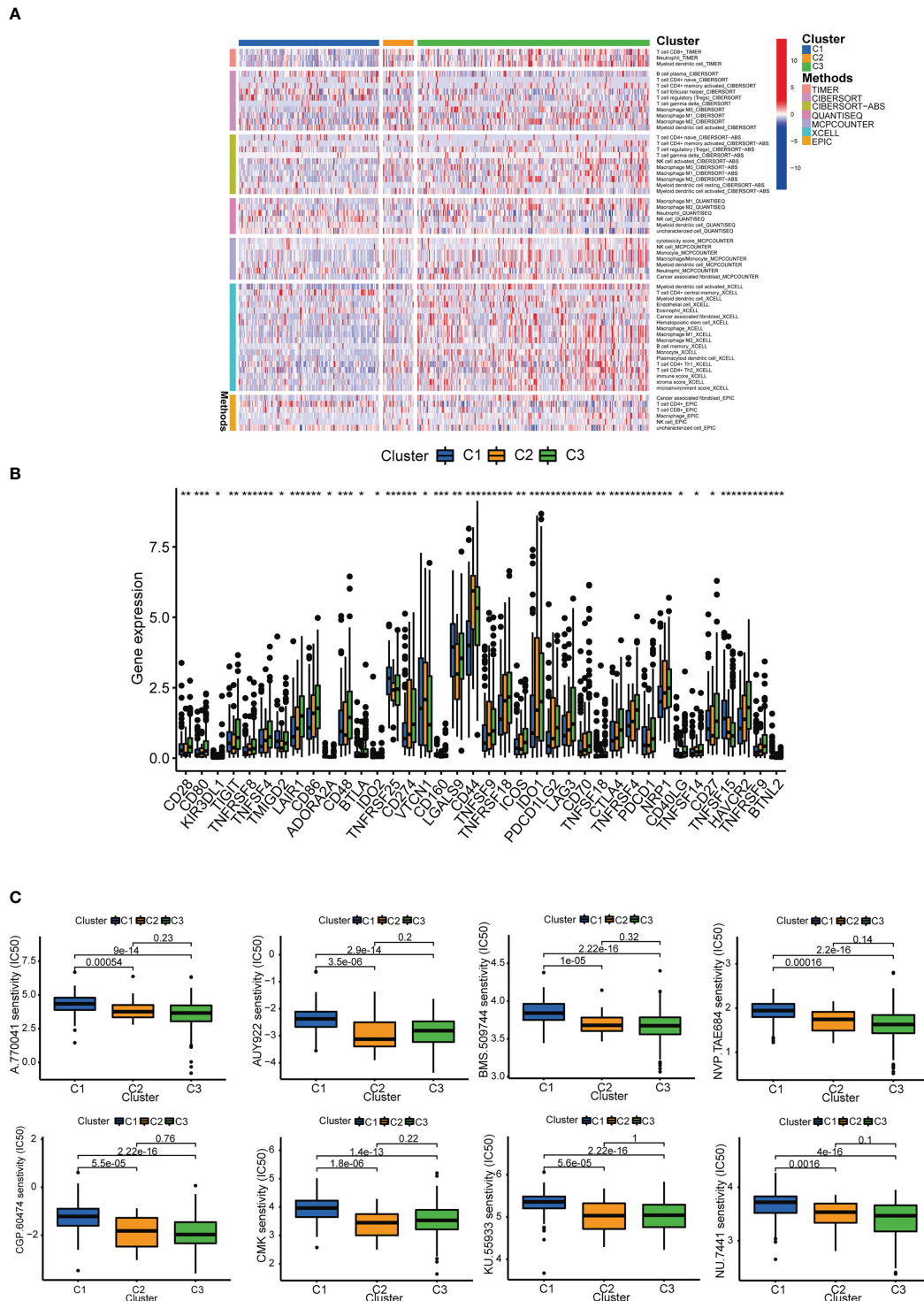


**FIGURE 12**  
 Prediction of immunotherapy efficacy. **(A)** Heatmap of immune cells in each cluster. **(B)** Differences in the expression of 18 immune checkpoints among the 3 clusters. **(C)** Immunotherapeutic agents that showed significantly different IC<sub>50</sub> among the 3 clusters. \*p<0.05, \*\*p<0.01, and \*\*\*p<0.001.

## 5 Conclusions

In summary, this study provides a valid model for prognosis prediction and clinical management of BLCA patients, thus

providing a reference for the development of individualized tumor therapy. Risk scores can predict the sensitivity of patients to chemotherapy. Inflammation-related lncRNAs can predict prognosis by identifying hot and cold tumors, and provide

therapeutic strategies, which will greatly improve the individualized therapy and patient prognosis. Understanding the mechanisms of inflammation-related lncRNAs in BLCA may provide new insights to treatment strategies for BLCA and other cancers.

## Data availability statement

The original contributions presented in the study are included in the article/Supplementary Material. Further inquiries can be directed to the corresponding authors.

## Ethics statement

Written informed consent was obtained from the individual(s) for the publication of any potentially identifiable images or data included in this article.

## Author contributions

PL designed the project and supervised the study. XX and LL contributed to the data analysis and original draft preparation. XX and CC conducted the experiments and revised the article. LL, XL, and MP reviewed and edited the manuscript. JY and WZ provided valuable suggestions for study. XW and HZ edited the language. All authors contributed to the article and approved the submitted version.

## References

1. Tang C, Liu H, Fan Y, He J, Li F, Wang J, et al. Functional nanomedicines for targeted therapy of bladder cancer. *Front Pharmacol* (2021) 12:778973. doi: 10.3389/fphar.2021.778973
2. Li K, Li S, Tang S, Zhang M, Ma Z, Wang Q, et al. KIF22 promotes bladder cancer progression by activating the expression of CDCA3. *Int J Mol Med* (2021) 48(6):211. doi: 10.3892/ijmm.2021.5044
3. Yang C, Jiang Y, Hao SH, Yan XY, Hong F, Naranmandura H. Aptamers: an emerging navigation tool of therapeutic agents for targeted cancer therapy. *J materials Chem B* (2021) 10(1):20–33. doi: 10.1039/D1TB02098F
4. Tang R, Xu J, Zhang B, Liu J, Liang C, Hua J, et al. Ferroptosis, necroptosis, and pyroptosis in anticancer immunity. *J Hematol Oncol* (2020) 13(1):110. doi: 10.1186/s13045-020-00946-7
5. Coussens LM, Werb Z. Inflammation and cancer. *Nature*. (2002) 420(6917):860–7. doi: 10.1038/nature01322
6. Murata M. Inflammation and cancer. *Environ Health Prev Med* (2018) 23(1):50. doi: 10.1186/s12199-018-0740-1
7. Giese MA, Hind LE, Huttenlocher A. Neutrophil plasticity in the tumor microenvironment. *Blood*. (2019) 133(20):2159–67. doi: 10.1182/blood-2018-11-844548
8. Rihawi K, Ricci AD, Rizzo A, Brocchi S, Marasco G, Pastore LV, et al. Tumor-related macrophages and inflammatory microenvironment in gastric cancer: Novel translational implications. *Int J Mol Sci* (2021) 22(8):3805. doi: 10.3390/ijms22083805
9. Atri C, Guerfali FZ, Laouini D. Role of human macrophage polarization in inflammation during infectious diseases. *Int J Mol Sci* (2018) 19(6):1801. doi: 10.3390/ijms19061801

## Funding

This study was supported by the National Natural Science Foundation of China (No.81770688), the Hubei Leading Talent Program in Medicine, and the Wuhan Application Foundation and Frontier Project (No. 2020020601012209), Wuhan Medical Research Project (NOWX21B04).

## Conflict of interest

The authors declare that the research was conducted in the absence of any commercial or financial relationships that could be construed as a potential conflict of interest.

## Publisher's note

All claims expressed in this article are solely those of the authors and do not necessarily represent those of their affiliated organizations, or those of the publisher, the editors and the reviewers. Any product that may be evaluated in this article, or claim that may be made by its manufacturer, is not guaranteed or endorsed by the publisher.

## Supplementary material

The Supplementary Material for this article can be found online at: <https://www.frontiersin.org/articles/10.3389/fonc.2023.972558/full#supplementary-material>

10. Lee K, Hwang H, Nam KT. Immune response and the tumor microenvironment: how they communicate to regulate gastric cancer. *Gut liver*. (2014) 8(2):131–9. doi: 10.5009/gnl.2014.8.2.131
11. Petersen CP, Meyer AR, De Salvo C, Choi E, Schlegel C, Petersen A, et al. A signalling cascade of IL-33 to IL-13 regulates metaplasia in the mouse stomach. *Gut*. (2018) 67(5):805–17. doi: 10.1136/gutjnl-2016-312779
12. Biswas SK, Mantovani A. Macrophage plasticity and interaction with lymphocyte subsets: cancer as a paradigm. *Nat Immunol* (2010) 11(10):889–96. doi: 10.1038/ni.1937
13. Ponting CP, Oliver PL, Reik W. Evolution and functions of long noncoding RNAs. *Cell*. (2009) 136(4):629–41. doi: 10.1016/j.cell.2009.02.006
14. Raponavoli NA, Qu K, Zhang J, Mikhail M, Laberge RM, Chang HY. A mammalian pseudogene lncRNA at the interface of inflammation and anti-inflammatory therapeutics. *eLife*. (2013) 2:e00762. doi: 10.7554/eLife.00762
15. Yao Y, Ma J, Xue Y, Wang P, Li Z, Liu J, et al. Knockdown of long non-coding RNA XIST exerts tumor-suppressive functions in human glioblastoma stem cells by up-regulating miR-152. *Cancer letters*. (2015) 359(1):75–86. doi: 10.1016/j.canlet.2014.12.051
16. Peinado H, Rafii S, Lyden D. Inflammation joins the "niche". *Cancer Cell* (2008) 14(5):347–9. doi: 10.1016/j.ccr.2008.10.012
17. McKiernan PJ, Molloy K, Cryan SA, McElvaney NG, Greene CM. Long noncoding RNA are aberrantly expressed *in vivo* in the cystic fibrosis bronchial epithelium. *Int J Biochem Cell Biol* (2014) 52:184–91. doi: 10.1016/j.biocel.2014.02.022
18. Pan W, Li W, Zhao J, Huang Z, Zhao J, Chen S, et al. lncRNA-PDPK2P promotes hepatocellular carcinoma progression through the PDK1/AKT/Caspase 3 pathway. *Mol Oncol* (2019) 13(10):2246–58. doi: 10.1002/1878-0261.12553

19. Wu H, Zhang ZY, Zhang Z, Xiao XY, Gao SL, Lu C, et al. Prediction of bladder cancer outcome by identifying and validating a mutation-derived genomic instability-related long noncoding RNA (lncRNA) signature. *Bioengineered*. (2021) 12(1):1725–38. doi: 10.1080/21655979.2021.1924555
20. Schober P, Boer C, Schwarte LA. Correlation coefficients: Appropriate use and interpretation. *Anesth Analgesia*. (2018) 126(5):1763–8. doi: 10.1213/ANE.0000000000002864
21. Friedman J, Hastie T, Tibshirani R. Regularization paths for generalized linear models via coordinate descent. *J Stat Software* (2010) 33(1):1–22. doi: 10.18637/jss.v033.i01
22. Liu L, Huang L, Chen W, Zhang G, Li Y, Wu Y, et al. Comprehensive analysis of necroptosis-related long noncoding RNA immune infiltration and prediction of prognosis in patients with colon cancer. *Front Mol Biosci* (2022) 9:811269. doi: 10.3389/fmolb.2022.811269
23. Pfaffl MW. A new mathematical model for relative quantification in real-time RT-PCR. *Nucleic Acids Res* (2001) 29(9):e45. doi: 10.1093/nar/29.9.e45
24. Shen Y, Peng X, Shen C. Identification and validation of immune-related lncRNA prognostic signature for breast cancer. *Genomics*. (2020) 112(3):2640–6. doi: 10.1016/j.ygeno.2020.02.015
25. Lin A, Qiu Z, Zhang J, Luo P. Effect of NCOR1 mutations on immune microenvironment and efficacy of immune checkpoint inhibitors in patient with bladder cancer. *Front Immunol* (2021) 12:630773. doi: 10.3389/fimmu.2021.630773
26. Wilkerson MD, Hayes DN. ConsensusClusterPlus: a class discovery tool with confidence assessments and item tracking. *Bioinformatics* (2010) 26(12):1572–3. doi: 10.1093/bioinformatics/btq170
27. Todenhöfer T, Seiler R. Molecular subtypes and response to immunotherapy in bladder cancer patients. *Trans andrology urology*. (2019) 8(Suppl 3):S293–s5. doi: 10.21037/tau.2019.06.21
28. Richters A, Aben KKH, Kiemeny L. The global burden of urinary bladder cancer: an update. *World J urology*. (2020) 38(8):1895–904. doi: 10.1007/s00345-019-02984-4
29. Li S, Liu X, Liu T, Meng X, Yin X, Fang C, et al. Identification of biomarkers correlated with the TNM staging and overall survival of patients with bladder cancer. *Front Physiol* (2017) 8:947. doi: 10.3389/fphys.2017.00947
30. Aggen DH, Drake CG. Biomarkers for immunotherapy in bladder cancer: a moving target. *J immunotherapy cancer*. (2017) 5(1):94. doi: 10.1186/s40425-017-0299-1
31. von der Maase H, Sengelov L, Roberts JT, Ricci S, Dogliotti L, Oliver T, et al. Long-term survival results of a randomized trial comparing gemcitabine plus cisplatin, with methotrexate, vinblastine, doxorubicin, plus cisplatin in patients with bladder cancer. *J Clin Oncol Off J Am Soc Clin Oncol* (2005) 23(21):4602–8. doi: 10.1200/JCO.2005.07.757
32. Crocetto F, Barone B, Ferro M, Busetto GM, La Civita E, Buonerba C, et al. Liquid biopsy in bladder cancer: State of the art and future perspectives. *Crit Rev oncology/hematology*. (2022) 170:103577. doi: 10.1016/j.critrevonc.2022.103577
33. Pan YH, Zhang JX, Chen X, Liu F, Cao JZ, Chen Y, et al. Predictive value of the TP53/PIK3CA/ATM mutation classifier for patients with bladder cancer responding to immune checkpoint inhibitor therapy. *Front Immunol* (2021) 12:643282. doi: 10.3389/fimmu.2021.643282
34. Zhao Z, Liu H, Zhou X, Fang D, Ou X, Ye J, et al. Necroptosis-related lncRNAs: Predicting prognosis and the distinction between the cold and hot tumors in gastric cancer. *J Oncol* (2021) 2021:6718443. doi: 10.1155/2021/6718443
35. Galon J, Bruni D. Approaches to treat immune hot, altered and cold tumours with combination immunotherapies. *Nat Rev Drug discovery*. (2019) 18(3):197–218. doi: 10.1038/s41573-018-0007-y
36. Duan Q, Zhang H, Zheng J, Zhang L. Turning cold into hot: Firing up the tumor microenvironment. *Trends cancer*. (2020) 6(7):605–18. doi: 10.1016/j.trecan.2020.02.022
37. Gajewski TF. The next hurdle in cancer immunotherapy: Overcoming the non-T-Cell-Inflamed tumor microenvironment. *Semin Oncol* (2015) 42(4):663–71. doi: 10.1053/j.seminoncol.2015.05.011
38. Zemek RM, De Jong E, Chin WL, Schuster IS, Fear VS, Casey TH, et al. Sensitization to immune checkpoint blockade through activation of a STAT1/NK axis in the tumor microenvironment. *Sci Trans Med* (2019) 11(501):eaav7816. doi: 10.1126/scitranslmed.aav7816
39. Sowers JL, Johnson KM, Conrad C, Patterson JT, Sowers LC. The role of inflammation in brain cancer. *Adv Exp Med Biol* (2014) 816:75–105. doi: 10.1007/978-3-0348-0837-8\_4
40. So AR, Si JM, Lopez D, Pellegrini M. Molecular signatures for inflammation vary across cancer types and correlate significantly with tumor stage, sex and vital status of patients. *PLoS One* (2020) 15(4):e0221545. doi: 10.1371/journal.pone.0221545
41. Oya Y, Hayakawa Y, Koike K. Tumor microenvironment in gastric cancers. *Cancer science*. (2020) 111(8):2696–707. doi: 10.1111/cas.14521
42. Feng Y, Wang J, Tan D, Cheng P, Wu A. Relationship between circulating inflammatory factors and glioma risk and prognosis: A meta-analysis. *Cancer Med* (2019) 8(17):7454–68. doi: 10.1002/cam4.2585
43. Greten FR, Grivennikov SI. Inflammation and cancer: Triggers, mechanisms, and consequences. *Immunity*. (2019) 51(1):27–41. doi: 10.1016/j.immuni.2019.06.025
44. Lucas C, Barnich N, Nguyen HTT. Microbiota, inflammation and colorectal cancer. *Int J Mol Sci* (2017) 18(6):1310. doi: 10.3390/ijms18061310
45. Jia G, Wang Y, Lin C, Lai S, Dai H, Wang Z, et al. LNCAROD enhances hepatocellular carcinoma malignancy by activating glycolysis through induction of pyruvate kinase isoform PKM2. *J Exp Clin Cancer research: CR*. (2021) 40(1):299. doi: 10.1186/s13046-021-02090-7
46. XiaYu K, GuoGang C, CanXuan L, WeiBin X. Comprehensive characterization of necroptosis-related lncRNAs in bladder cancer identifies a novel signature for prognosis prediction. *Dis markers*. (2022) 2022:2360299. doi: 10.1155/2022/2360299
47. Luo D, Liu Y, Yuan S, Bi X, Yang Y, Zhu H, et al. The emerging role of NR2F1-AS1 in the tumorigenesis and progression of human cancer. *Pathology Res practice*. (2022) 235:153938. doi: 10.1016/j.prp.2022.153938
48. He SL, Chen YL, Chen QH, Tian Q, Yi SJ. lncRNA KCNQ1OT1 promotes the metastasis of ovarian cancer by increasing the methylation of EIF2B5 promoter. *Mol Med* (2022) 28(1):112. doi: 10.1186/s10020-022-00521-5
49. Crocetto F, Cimmino A, Ferro M, Terracciano D. Circulating tumor cells in bladder cancer: a new horizon of liquid biopsy for precision medicine. *J basic Clin Physiol Pharmacol* (2022) 33(5):525–7. doi: 10.1515/jbcp-2021-0233
50. Ma M, Pei Y, Wang X, Feng J, Zhang Y, Gao MQ. lncRNA XIST mediates bovine mammary epithelial cell inflammatory response via NF- $\kappa$ B/NLRP3 inflammasome pathway. *Cell proliferation*. (2019) 52(1):e12525. doi: 10.1111/cpr.12525